# Structural Consequences of Histidine Phosphorylation: NMR Characterization of the Phosphohistidine Form of Histidine-Containing Protein from *Bacillus subtilis* and *Escherichia coli*†

Ponni Rajagopal,‡ E. Bruce Waygood,§ and Rachel E. Klevit*,‡

*Department of Biochemistry, SJ-70, University of Washington, Seattle, Washington 98195, and Department of Biochemistry, University of Saskatchewan, Saskatoon, Saskatchewan, S7N 0W0, Canada*

*Received October 6, 1994; Revised Manuscript Received November 8, 1994*®

ABSTRACT: The bacterial phosphoenolpyruvate:sugar phosphotransferase system involves a series of reactions in which phosphoprotein intermediates are formed. Histidine-containing protein (HPr) is phosphorylated on the $N^{\delta 1}$ position of the imidazole ring of His15 by enzyme I and acts as a phosphoryl donor to the sugar-specific enzymes IIA. The structure of phosphorylated HPr from *Bacillus subtilis*, primarily, and from *Escherichia coli* has been studied by nuclear magnetic resonance (NMR) spectroscopy. Phosphorylation of His15 results in large downfield shifts in amide proton and nitrogen resonances for residues 16 and 17 but results in only modest or no shifts in other backbone resonances. The exchange rates of these two amide groups are decreased more than 10-fold upon phosphorylation. Analysis of the coupling constants $^3J_{NH\alpha}$ revealed no significant changes throughout the protein, indicating that backbone $\phi$ dihedral angles do not change detectably. $^3J_{\alpha\beta}$ and $^3J_{N\beta}$ patterns determined from P.E.COSY and HNHB spectra, respectively, revealed a change in one side chain, that of conserved Arg17. Analysis of NOESY spectra revealed a limited number of changes in NOEs involving protons in Ser12, His15, Arg17, and Pro18 in *B. subtilis* HPr. The NMR results indicate that the Arg17 side chain becomes limited in its conformational range in the phosphorylated protein, taking on a conformation that points its guanidinium group toward the phosphoryl group on His15. In addition, the tautomeric and ionization states of His15 have been determined using $^{15}N$ and $^{31}P$ NMR. At neutral pH, the imidazole is predominantly in the protonated form and the phosphoryl group is in the dianionic form in P-His15. Altogether, the results indicate that phosphorylation of His15 yields only a local effect on the protein's structure. The data are consistent with a small change in the disposition of the histidine side chain, allowing phosphoryl group oxygens to serve as hydrogen bond acceptors for the amide protons of residues Ala16 and Arg17, which constitute the first two residues of an α-helix. Thus, similar to many proteins that bind phosphoryl moieties noncovalently, the phosphoryl group in P-His15-HPr is situated to allow for a favorable electrostatic interaction at the N-terminal end of an α-helix.

Although not as common as serine, threonine, and tyrosine phosphorylation, a number of reports of histidine phosphorylation have appeared in recent years. Both histidine kinases and histidine phosphatases have been described (Hughes 1994; Motojima & Goto, 1994), but there is less information available concerning substrates of histidine phosphorylation. Both nitrogens in imidazole can be phosphorylated in solution, and the target nitrogen in a given substrate must be governed by specific structural features. The bacterial phosphoenolpyruvate:sugar phosphotransferase system (PTS),[1] shown in Scheme 1, offers examples of both types of histidine phosphorylation: enzymes I and IIA are each phosphorylated on a histidine $N^{\epsilon 2}$ while HPr and some IIBs are phosphorylated on a histidine $N^{\delta 1}$ [see Postma *et al.* (1993) for a thorough review]. Thus, the PTS is a rich system in which to study proteins that undergo histidine phosphorylation and the effects of such phosphorylation on protein structure.

Scheme 1

$$\text{phosphoenolpyruvate} + \text{enzyme I} \rightleftharpoons \text{P-enzyme I} + \text{pyruvate}$$

$$\text{P-enzyme I} + \text{HPr} \rightleftharpoons \text{P-HPr} + \text{enzyme I}$$

$$\text{P-HPr} + \text{IIA}^{\text{sugar}} \rightleftharpoons \text{P-IIA}^{\text{sugar}} + \text{HPr}$$

$$\text{P-IIA}^{\text{sugar}} + \text{IIB}^{\text{sugar}} \rightleftharpoons \text{P-IIB}^{\text{sugar}} + \text{IIA}^{\text{sugar}}$$

$$\text{P-IIB}^{\text{sugar}} + \text{sugar}_{\text{out}} \xrightleftharpoons{\text{IIC}^{\text{sugar}}} \text{sugar-P}_{\text{in}} + \text{IIB}^{\text{sugar}}$$

The PTS catalyzes the phosphorylation and transport of a number of sugars in both Gram-positive and Gram-negative

† This work was supported by NIH Grant RO1 DK35187 and an American Heart Association Established Investigatorship (R.E.K.) and by MRC Operating Grant MT6147 (E.B.W.).

* To whom correspondence should be addressed (telephone, 206-543-5891; FAX, 206-543-8394; E-mail, klevit@u.washington.edu).

‡ University of Washington.

§ University of Saskatchewan.

® Abstract published in *Advance ACS Abstracts,* December 1, 1994.

[1] Abbreviations: HPr, histidine-containing protein; *bs*HPr, *Bacillus subtilis* HPr; *ec*HPr, *Escherichia coli* HPr; EI, enzyme I; EIIA, enzyme IIA; PTS, phosphoenolpyruvate:sugar phosphotransferase system; 2D and 3D, two and three dimensional; NOESY, nuclear Overhauser enhancement spectroscopy; HSQC, heteronuclear single-quantum correlation; HMQC, heteronuclear multiple-quantum correlation; TOCSY, total correlation spectroscopy; PEP, phosphoenolpyruvate; P.E.COSY, primitive-exclusive coherence spectroscopy.

0006-2960/94/0433-15271$04.50/0 

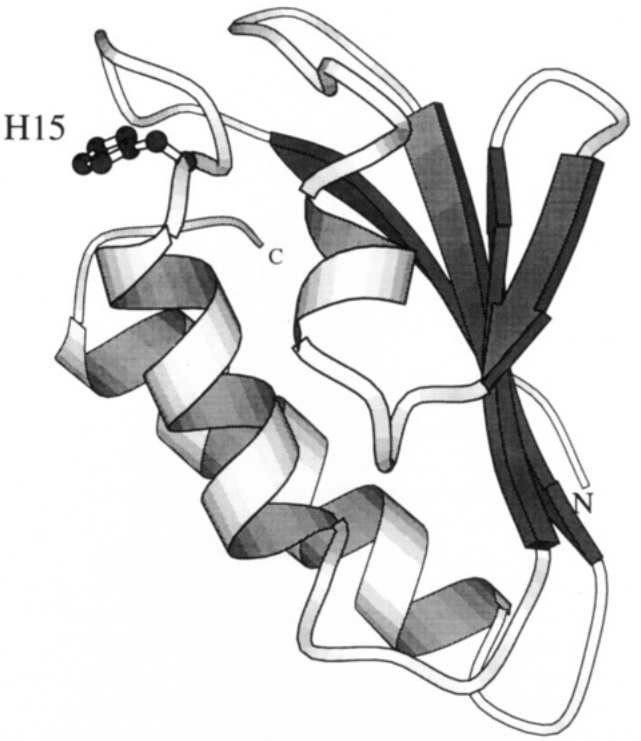


FIGURE 1: Ribbon representation of the folding topology of *bs*HPr. In the foreground, the side chain of His15 is shown in its position atop the first α-helix. The image was prepared using MOLSCRIPT (Kraulis, 1991).

bacteria. As illustrated in Scheme 1, transfer of a phosphoryl group from phosphoenolpyruvate to a sugar molecule proceeds via a series of phosphoprotein intermediates. Histidine-containing protein (HPr) is the phosphoryl acceptor from enzyme I (EI) and the phosphoryl donor to enzyme IIA (EIIA). HPrs from Gram-negative and Gram-positive organisms share 33−66% sequence identity; NMR and X-ray diffraction studies have confirmed that HPrs from a variety of microorganisms share a common tertiary fold (Klevit & Waygood, 1986; Hammen *et al.*, 1991; Van Nuland *et al.*, 1992, 1994; Kalbitzer *et al.*, 1991; Kalbitzer & Hengstenberg, 1993; Wittekind *et al.*, 1990, 1992; Herzberg *et al.*, 1992; Jia *et al.*, 1993a,b, 1994). The fold of HPr consists of a four-stranded antiparallel β-sheet with two to three α-helices on one face of the sheet (see Figure 1). His15, the site of phosphorylation, is on a loop connecting the first β-strand and the first α-helix, in the so-called helix N-cap position.

In spite of their similarities, HPrs are not efficiently interchangeable in heterologous systems, indicating that specific aspects of each HPr species are critical for the protein−protein interactions that accompany phosphotransfer (Reizer *et al.*, 1992). Well-defined three-dimensional structures are therefore required to identify the subtle, yet critical differences between HPr species that result in their specificities. The structure of HPr in its phosphorylated form is also required. Even in the absence of enzyme IIA, however, the half-life of P-His15-HPr is only minutes due to nonenzymatic hydrolysis of the phosphoramidate bond. Fortunately, P-His15-HPr can be maintained in the NMR for several days using an *in situ* regeneration system (Wittekind & Klevit, 1991). Here we characterize the phosphohistidine-containing form of HPr using $^{1}H$, $^{15}N$, and $^{31}P$ NMR spectroscopy.

## MATERIALS AND METHODS

*Protein Purification.* Overexpression and purification of *ec*HPr and *bs*HPr have been described previously (Sutrina *et al.*, 1990; Wittekind *et al.*, 1990; Hammen *et al.*, 1991). Enzyme I and the *ec*HPr mutant Arg17Lys were obtained from *Escherichia coli* (Anderson *et al.*, 1993), and *Bacillus subtilis* enzyme I was obtained as described (Reizer *et al.*, 1992). Proteins uniformly enriched with $^{15}N$ were obtained by growing transformed *E. coli* strains on [$^{15}N$]$NH_4Cl$.

*NMR Sample Preparation.* Samples used for NMR experiments were dialyzed extensively against the appropriate buffer. Sample pH was measured in the NMR tube with an electrode from Microelectrodes, Inc., and was adjusted using HCl or NaOH (as appropriate). Sample pH values are cited as direct meter readings and are not corrected for isotope effects. The protein concentration of the samples ranged from 1 to 2 mM.

P-His15-HPr was generated *in situ* in buffer containing 100 mM phosphate, 70 mM phosphoenolpyruvate (PEP), 4 mM dithiothreitol, 2 mM $MgCl_2$, and enzyme I (5 units).

In order to slow the rate of phosphohydrolysis, spectra were collected at pH 7.4 and 22 °C, unless stated otherwise. Although phosphohydrolysis is even slower at higher pH values, backbone amide exchange rates increase with pH, degrading the quality of the NMR data collected. Therefore, the conditions used represent a compromise between phosphohydrolysis effects and amide exchange effects. Since these conditions are different from those used in our earlier studies of unphosphorylated HPrs (Klevit *et al.*, 1986; Wittekind *et al.*, 1990, 1992; Hammen *et al.*, 1991), control spectra were collected for every experiment. To account for any potential effects due to the presence of the regeneration system, control spectra were collected on samples of unphosphorylated HPr dissolved in regeneration buffer (see above), and spectra of P-His15-HPr were then collected following the addition of EI. Under the conditions used for the NMR experiments, P-His15-HPr is in slow exchange with HPr; therefore, when detectable concentrations of HPr built up during the course of an experiment, its resonances were detected as separate peaks, rather than contributing to an average resonance position. This behavior greatly facilitated the analysis of P-His15-HPr since the $^{1}H$ and $^{15}N$ resonances of unphosphorylated HPr have been previously assigned (Hammen *et al.*, 1991; Wittekind *et al.*, 1992; van Nuland *et al.*, 1993).

*NMR Spectroscopy.* NMR experiments were performed on a Bruker AM500 or DMX500 NMR spectrometer. All spectra were acquired at 22 °C and pH 7.4 unless otherwise noted. Recycle delays of 1.5 s were used in all the experiments. Presaturation was used to suppress the $H_2O$ resonance, except in the experiments used to measure exchange rates, where the 1-$\bar{1}$ echo pulse sequence (Sklenar & Bax, 1987) was used. The States−TPPI method (Marion *et al.*, 1989) was used to achieve quadrature detection in $t_1$ in the HNHB experiment, the States method (States *et al.*, 1982) was used in the P.E.COSY experiment (Mueller, 1987), and TPPI (Marion & Wüthrich, 1983) was used otherwise.

2D homonuclear experiments (NOESY, TOCSY, and P.E.COSY) were collected with standard pulse sequences. Spectra were acquired with 2K complex points with spectral widths of either 10 000 or 6578 Hz. A total of 600 $t_1$s were

collected for NOESY and TOCSY spectra, with 64 transients per $t_1$. NOESY (Bodenhausen *et al.*, 1984) spectra were recorded at two different mixing times, 75 and 150 ms. TOCSY (Bax & Davis, 1985) spectra were recorded with a spin−lock mixing period of 75 ms. P.E.COSY spectra were acquired with 32 transients per $t_1$ for a total of 400 $t_1$s (Mueller, 1987).

2D ($^1$H,$^{15}$N)-HMQC or -HSQC spectra (Bax *et al.*, 1990) were acquired with 32 or 64 transients per $t_1$ value. The acquisition time was 102.4 ms in $t_2$ and was usually 64 ms in $t_1$. A delay of 4.3 ms ($<1/2J_{NH}$) or 2.3 ms ($<1/4J_{NH}$) was used for chemical shift refocusing and for the evolution of $^1J_{NH}$ couplings in HMQC or HSQC spectra. The $^1$H and $^{15}$N transmitters were set to 4.6 and 114.2 ppm, respectively. $^1$H decoupling in $t_1$ was achieved with a 180° pulse in the middle of $t_1$, and $^{15}$N decoupling in $t_2$ was achieved via GARP modulation of a 2.3−kHz rf field. $^3J_{NH\alpha}$ coupling constants were measured from ($^1$H,$^{15}$N)-HMQC-*J* spectra collected with an acquisition time of 140 ms in $t_1$. A 2D version of the HNHB experiment (Archer *et al.*, 1991) was performed with the following parameters: 300 complex $t_1$s with 64 transients per $t_1$, 1 K complex points in $t_2$, and a spectral width of 7002 Hz.

The tautomeric states of the histidine ring were determined from ($^1$H,$^{15}$N)-HMQC-*J* experiments (Van Dijk *et al.*, 1992; Pelton *et al.*, 1993) using a delay of 22 ms to refocus chemical shifts and to allow the long-range coupling between the carbon-bound ring protons and the imidazole nitrogens to evolve. In the $^{15}$N dimension, the carrier was placed at 200 ppm.

A series of ($^1$H,$^{15}$N)-HMQC spectra were acquired at different time intervals whereby the first time point was begun 5 min after dissolution of the lyophilized protein in $D_2O$ (pH 7.4). The experiments were collected using an external timer device (AM TIMER, Tschudin Associates, Kensington, MD) to reduce disk read/write time at the end of each $t_1$ experiment. A total of 128 $t_1$s with 4 transients per $t_1$ were acquired, and an entire 2D spectrum could be collected in 20 min. The experiments were performed on the phosphorylated sample after confirmation that lyophilization did not cause dephosphorylation of the protein.

The exchange rates of the fast-exchanging amide protons were measured following the method of Spera *et al.* (1991). In this method, ($^1$H,$^{15}$N)-HMQC spectra with and without water presaturation were recorded at 30 °C at four different pH values: 6.9, 7.2, 7.6, and 8.3. The 1-$\bar{1}$ echo pulse sequence was used to suppress $H_2O$ in the spectra taken without presaturation. Volume integrals and/or peak heights were measured for all amide proton cross peaks. Ratios of the intensities, $M_0/M_{ps}$, were computed for each cross peak, where $M_0$ is the cross peak intensity in a spectrum acquired without presaturation and $M_{ps}$ is the intensity of the cross peak in a spectrum taken with presaturation. Exchange rates were computed from $M_0/M_{ps}$ ratios as outlined in Spera *et al.* (1991).

$^1$H spin−lattice relaxation rates were measured as described in Peng *et al.* (1992) using $^{15}$N-relayed NOESY spectra. A series of spectra were acquired with NOE mixing delays of 5, 10, 20, 40, 80, and 160 ms. $^1$H spin−lattice relaxation rates were obtained by fitting the measured amide cross-peak intensities to an exponential decay.

$^{15}$N and $^{31}$P resonances were directly observed using a 5 mM broad-band probe. For $^{15}$N, a spectral width of 20 000 Hz was used and the carrier was set to 200 ppm. No proton decoupling was applied and 2000−4000 transients were acquired.

Data were processed using Felix 2.3 (Biosym Technologies, Inc). Data were apodized in both $t_1$ and $t_2$ dimensions with a squared sine bell shifted by 45° or 65°. Data were zero-filled to 1 K complex points before apodization in the $t_1$ dimension. $^3J_{\alpha\beta}$ coupling constants were measured from P.E.COSY spectra after zero-filling in the $t_1$ dimension to 4K points, yielding a digital resolution of 1.2 Hz/point. Chemical shifts were referenced to $H_2O$ (4.71 ppm, 22 °C) and external liquid ammonia ($^{15}$N).

*Model Building.* A model of P-His15-HPr was built on the basis of the coordinates of *bs*HPr (PDB code 2HPR), using the software package INSIGHT (Biosym, Inc.). A phosphoryl group was added to His15, and a bond formed between the $N^{\delta 1}$ atom and the phosphorus atom. A rotation of ~15° about $X_2$ of His15 was performed to relieve unfavorable nonbonded contacts involving the phosphoryl group. No other adjustments were made to the model.

## RESULTS

*Effects of Phosphorylation of His15 on Backbone Chemical Shifts.* The half-life of P-His15-HPr in solution at pH 6.5 and 37 °C is ~5 min due to facile hydrolysis of the phosphoramidate bond (Waygood *et al.*, 1985; Anderson *et al.*, 1992). Fortunately, it is possible to maintain a steady-state concentration of P-His15-HPr by using an *in situ* enzymatic regeneration system that includes a catalytic amount of EI and high concentrations of PEP (Wittekind & Klevit, 1991; see Materials and Methods). Figure 2 shows a ($^1$H,$^{15}$N)-HSQC spectrum of P-His15-HPr superimposed on that of HPr from *B. subtilis* (*bs*HPr). The most striking aspect of the spectra is that the majority of resonances are not detectably perturbed by phosphorylation. With the exception of the resonances for residues 16 and 17, the chemical shift changes are small and the amide resonances could be assigned by comparison to the spectrum of unphosphorylated HPr. To confirm this, and to unambiguously assign the resonances for Ala16 and Arg17, P-His15-*bs*HPr was assigned directly using a variety of 2D homonuclear and heteronuclear ($^1$H,$^{15}$N) experiments (data not shown). The amide resonances for Ala16 and Arg17 are each shifted downfield by about 1 and 3 ppm in the $^1$H and $^{15}$N dimensions, respectively, on phosphorylation. Analogous HSQC spectra were collected for unphosphorylated and phosphorylated HPr from *E. coli* (*ec*HPr), which shares 34% sequence identity with the *B. subtilis* protein. The results were very similar, with the cross peaks for Thr16 and Arg17 showing analogous downfield chemical shift perturbations (data not shown). We have performed the majority of our experiments on *bs*HPr but will report here some results on *ec*HPr as well since we believe that the general conclusions are the same for the two related proteins.

Amide resonances with chemical shift changes of more than a line width [>20 Hz (0.04 ppm) for $^1$H and >5 Hz (0.1 ppm) for $^{15}$N] on phosphorylation are listed in Table 1. Residues near His15, extending into the beginning of α-helix A (which consists of residues 16−28), each experience combined ($^1$H + $^{15}$N) absolute shifts of >25 Hz. Smaller perturbations are observed for residues between 42 and 62 and in α-helix C (residues 79−85) in both phosphorylated

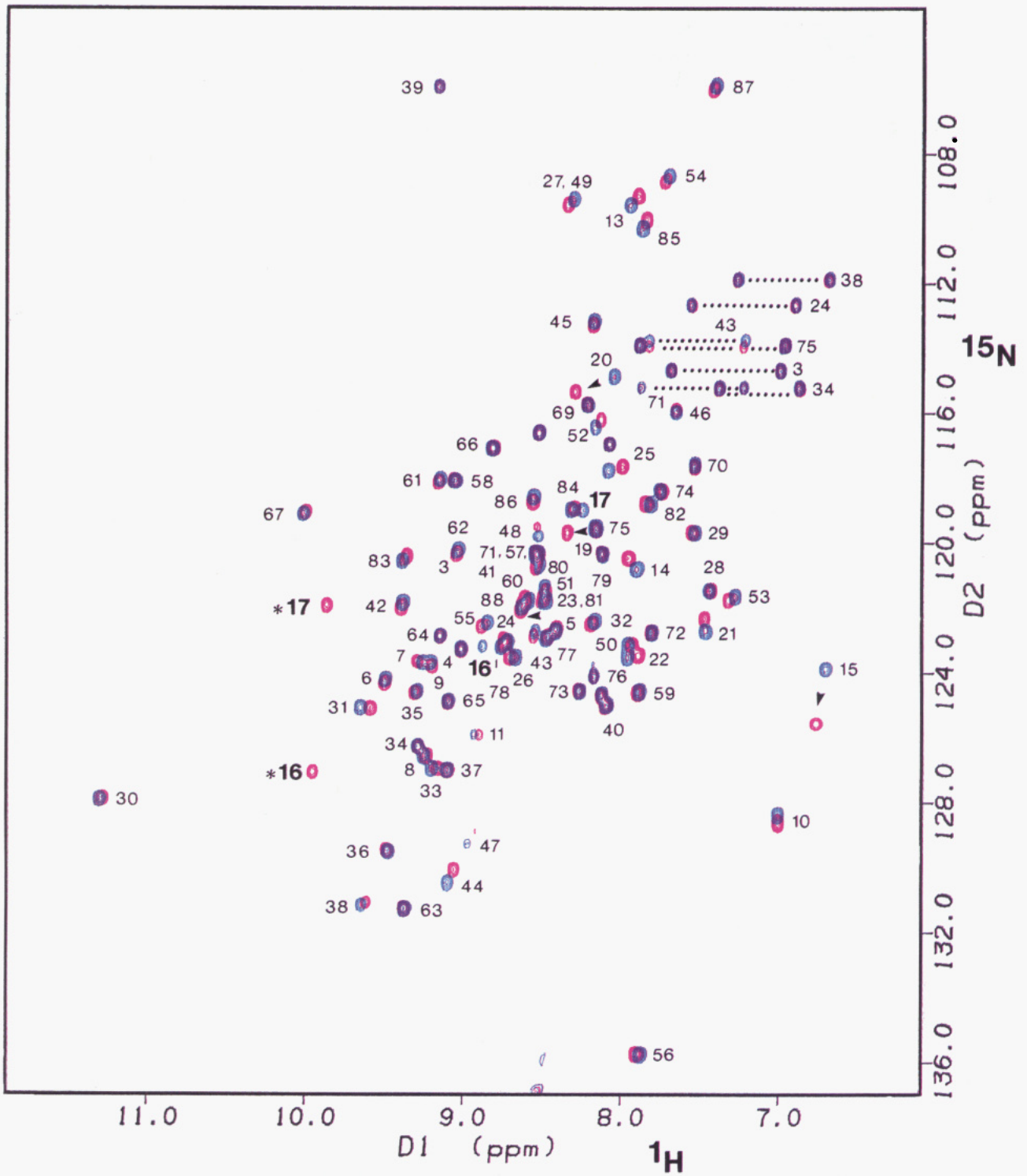


FIGURE 2: ($^1$H,$^{15}$N)-HSQC spectrum of P-His15-*bs*HPr (red) shown overlaid on that of *bs*HPr (blue). The spectra were collected at pH 7.4 and 22 °C. Resonances are labeled at their positions in unphosphorylated HPr. Side-chain amide protons are shown connected by dotted lines. Resonances that shift more than 50 Hz are indicated with arrows. Resonances of NH16 and NH17 are indicated in bold type, and the new positions of NH16 and NH17 are also indicated by an asterisk.

proteins. Intriguingly, small but reproducible perturbations occur near the site of regulatory phosphorylation, Ser 46, in *bs*HPr whereas none were observed in *ec*HPr.

*Effects of Phosphorylation on Amide Exchange Rates.* The large downfield shifts observed for the amide resonances of *bs*HPr residues Ala16 and Arg17 could be indicative of their involvement in new H-bonds in P-His15-HPr. In general, hydrogen-bonded amide protons exhibit slower exchange rates with solvent than their non-hydrogen-bonded counterparts. Therefore, we compared this property in the two forms. Due to the rapid rate of phosphohydrolysis of P-His15-HPr at pH values below neutral, the H−D exchange experiments had to be performed at pH 7.4 where amide exchange rates are quite fast (Wüthrich, 1986). In conventional H−D exchange experiments, the same set of slowly exchanging cross peaks was detected for both forms in ($^1$H,$^{15}$N)-HMQC spectra collected during the first 25 min following dissolution of the samples in $D_2O$. The cross peaks for Ala16 and Arg17 were not detected, indicating that their lifetimes are too short to be detected in the H−D exchange

Table 1: Amide Resonance Chemical Shift Perturbations Observed for P-His15-*bs*HPr

| residue | $^1$H (ppm)[a] | $^{15}$N (ppm)[a] | ($^1$H + $^{15}$N) (Hz)[b] |
|---|---|---|---|
| Val8 | 0.04 | 0.01 | 21 |
| Ala10 | 0.01 | −0.23 | 17 |
| Ser12 | −0.03 | −0.70 | 51 |
| Gly13 | 0.07 | 0.33 | 52 |
| His15 | −0.10 | −1.73 | 138 |
| Ala16 | −1.02 | −3.48 | 686 |
| Arg17 | −1.48 | −2.46 | 865 |
| Ala19 | −0.14 | −0.23 | 82 |
| Thr20 | −0.22 | −0.42 | 131 |
| Leu22 | 0.07 | 0.07 | 39 |
| Val23 | −0.11 | −0.26 | 68 |
| Thr25 | 0.07 | 0.07 | 39 |
| Val42 | −0.01 | −0.19 | 15 |
| Asn43 | 0.01 | −0.15 | 13 |
| Leu44 | 0.04 | 0.35 | 38 |
| Ile47 | 0.07 | 0.53 | 62 |
| Met48 | 0.01 | 0.22 | 16 |
| Ser52 | 0.05 | 0.26 | 38 |
| Thr62 | 0.01 | −0.17 | 14 |
| Gly85 | 0.02 | 0.23 | 22 |

[a] Difference calculated as $\delta$(HPr) − $\delta$(P-His15-HPr). [b] The magnitude of the chemical shift differences observed for $^1$H and $^{15}$N (in hertz) were added together.

experiment at this pH. Protons with lifetimes that are shorter than a few minutes will not be detected in this experiment.

Amide exchange rates of rapidly exchanging amide protons were measured using a method that takes advantage of saturation transfer from the solvent (Spera *et al.*, 1991). This technique allows for the determination of very fast exchange rates but becomes insensitive for exchange rates slower than 1 $s^{-1}$ under the conditions used. Only a few amide protons that were not observed in the first time point in an H−D experiment in $D_2O$ at pH 7.4 exhibit differential exchange rates that can be measured with confidence in the two forms of HPr. The largest differences are observed for the amide protons of Ala16 and Arg17, $k_{ex}$ (pH 7.4) = 11 $s^{-1}$ and 14 $s^{-1}$ in *bs*HPr, respectively, whereas in P-His15-*bs*HPr both amides exchange with $k_{ex}$ (pH 7.4) < 1 $s^{-1}$. Thus, the exchange rates of these two amide protons in P-His15-HPr fall between the rates that can be measured accurately by either of the two types of exchange experiments. Nevertheless, the exchange rates of NH16 and NH17 are decreased at least 10-fold relative to unphosphorylated HPr. Together, the decrease in exchange rate and large downfield shifts observed for these two amide groups are strong evidence for their involvement in new H-bonds in P-His15-HPr.

The amide exchange rates of *bs*HPr residues Ser12 and Gly13 near the active site are also decreased on phosphorylation. Ser12 exchanges so rapidly in the unphosphorylated form that its amide cross peak is not observed under the conditions used. The Ser12 cross peak is observed in spectra of P-His15-HPr, and its exchange rate is 120 $s^{-1}$. The exchange rate for Gly13 decreases from 2.6 to <1 $s^{-1}$. In contrast, there is no change in exchange rate for the amide proton of His15 over the pH range studied.

*Effects of Phosphorylation on the Structure of bsHPr.* The surprisingly limited nature of the backbone amide chemical shift perturbations observed upon phosphorylation suggested that any structural changes were likely to be fairly small and localized. Therefore, careful comparisons of a number of different spectra were performed. Matched ($^1$H,$^{15}$N)-HMQC-*J* spectra were collected to detect differences in $^3J_{NH\alpha}$ coupling constants that would indicate changes in backbone conformation. All coupling constants that could be measured in both forms (81 of 81 total) agreed within 1 Hz between the two forms. The His15 amide cross peak is quite broad in spectra of P-His15-HPr, most likely due to the fact that spectra were collected at pH values close to the imidazolium p$K_a$. Therefore, it is difficult to make definitive conclusions concerning the backbone coupling constant for His15 in P-His15-HPr. Otherwise, the data indicate that no detectable changes in backbone $\phi$ dihedral angles occur upon His15 phosphorylation.

Table 2: Differences Observed in NOEs between *bs*HPr and P-His15-*bs*HPr

| NOE observed | *bs*HPr | P-His15-*bs*HPr |
|---|---|---|
| His15 $C^\delta$H−Ser12 $C^\beta$H | medium | medium |
| His15 $C^\delta$H−Ser12 $C^{\beta'}$H | medium | weak |
| His15 $C^\delta$H−His15 NH | $i$[a] | $2i$[a] |
| His15 $C^\delta$H−His15 $C^\beta$H | weak | medium |
| His15 $C^\delta$H−His15 $C^{\beta'}$H | medium | medium |
| His15 $C^\epsilon$H−Pro18 $C^{\gamma,\gamma'}$H[b] | medium | absent |
| His15 $C^\epsilon$H−Arg17 $C^{\beta,\beta'}$H | absent | medium |
| Arg17 $C^{\delta,\delta'}$H−Arg17 $C^{\beta,\beta'}$H | absent | medium |
| Arg17 $C^\alpha$H−Thr20 $C^\beta$H | absent | medium |

[a] $i$ = intensity of cross peak. [b] Prochiral proton resonances that are poorly resolved are denoted as $C^{\beta,\beta'}$H, $C^{\gamma,\gamma'}$H, etc.

Two types of spectra that correlate with side-chain conformation were collected. $^3J_{\alpha\beta}$ constants were determined from P.E.COSY spectra. Of the 25 $^3J_{\alpha\beta}$ constants that could be measured, no significant differences were detected, even in His15 itself.[2] ($^1$H,$^{15}$N)-HNHB spectra were collected in order to obtain coupling information for residues whose H$\alpha$−H$\beta$ cross peaks are badly overlapped in P.E.COSY spectra. Coupling patterns could be discerned for an additional 11 residues in the HNHB spectrum.[2] Only the resonance corresponding to Arg17 showed a difference in its pattern between the two forms. No HNHB cross peaks are present for Arg17 in the spectrum of unphosphorylated HPr.[3] This result could be due either to the side chain existing in the rotamer conformation in which $X_1$ = 180° (*trans*) or to the side chain being conformationally averaged. Although these two possibilities can be distinguished by $^3J_{\alpha\beta}$, the relevant cross peaks for Arg17 are badly overlapped in the COSY spectrum. In contrast, the HNHB spectrum of P-His15-HPr contains a cross peak for Arg17. This observation indicates that Arg17 exists mainly in a single rotamer conformation, with $X_1$ = either 60° ($g^-$) or 300° ($g^+$). Again, the two possibilities are distinguishable by $^3J_{\alpha\beta}$, but the COSY cross peaks are still not well resolved. Nevertheless, the results indicate a significant change in the side chain of Arg17, from being conformationally averaged or having a $X_1$ = 180° to a single rotamer that is close to $X_1$ = either 60° or 300°.

[2] *bs*HPr residues for which $^3J_{\alpha\beta}$ constants could be measured in both forms are Gln3, Lys4, Phe6, Ser12, His15, Pro18, Leu22, Gln24, Lys28, Tyr29, Asp32, Asn34, Leu35, Glu36, Tyr37, Asn38, Lys40, Ser46, Ser52, Ser64, Asp69, Asp72, Glu78, Ser83, and Glu88. Residues not in the preceding list for which HNHB cross peaks were observed are Lys7, Arg17, Ser27, Leu44, Lys57, Glu60, Glu70, Leu77, Met81, Glu84, and Leu86.

[3] The intensity of HNHB cross peaks can be affected by amide exchange rates, leading to the possibility that an HNHB peak is not observed for Arg17 in unphosphorylated HPr due to its rapid exchange rate. However, HNHB peaks were observed for several amides with exchange rates similar to or faster than that of Arg17, effectively ruling out this possibility.

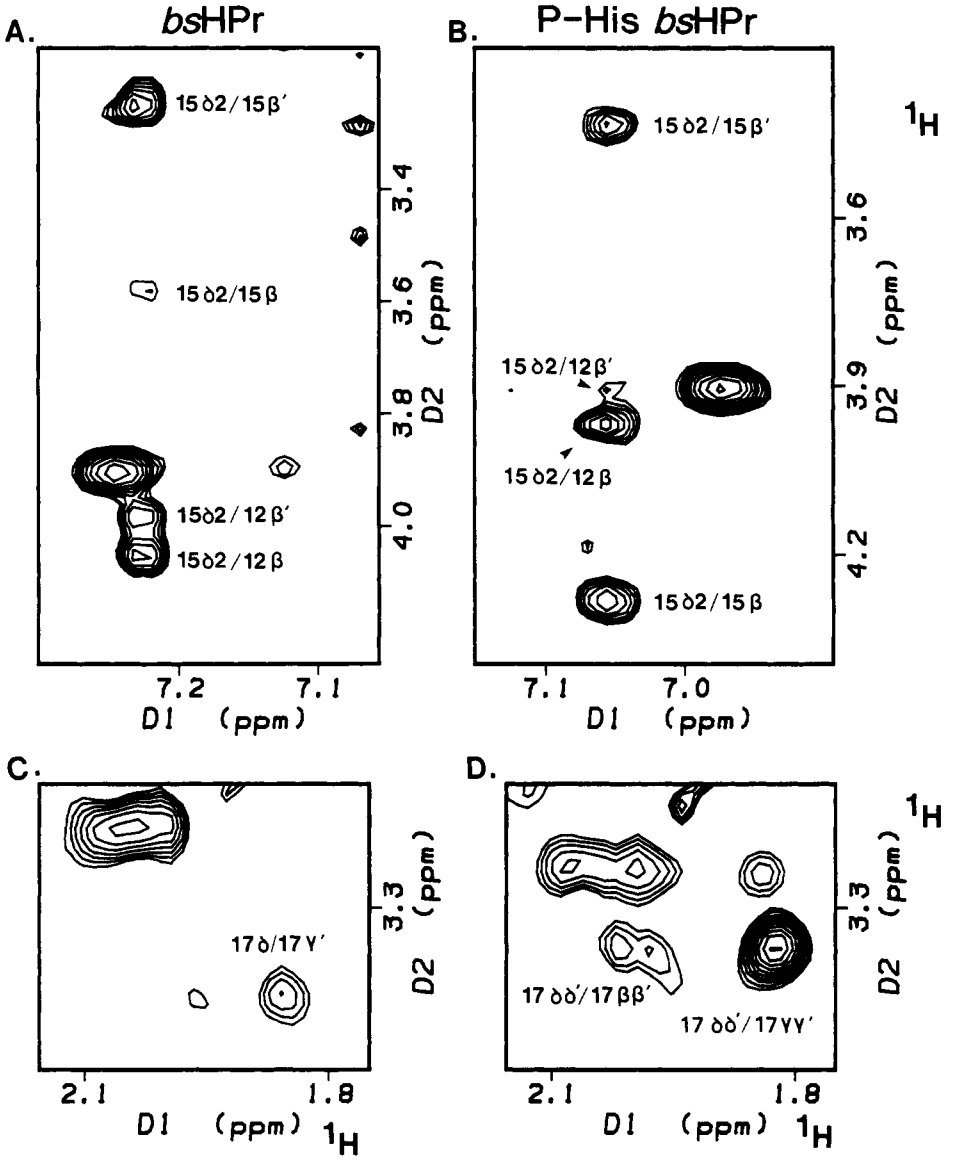


FIGURE 3: Regions of 2D NOESY spectra of *bs*HPr and P-His15-*bs*HPr at 22 °C and pH 7.4: A, NOEs from the His15 $H^{\delta 2}$ proton in *bs*HPr; B, NOEs from the His15 $H^{\delta 2}$ proton in P-His15-*bs*HPr; C, intraresidue NOEs from Arg17$C^{\delta}$ protons in *bs*HPr; D, intraresidue NOEs from Arg17$C^{\delta}$ protons in P-His15-*bs*HPr.

2D $^1$H NOESY spectra were collected using short mixing times for both forms of *bs*HPr and compared peak by peak. A limited number of differences were detected, many of which involve protons near His15. These are listed in Table 2, and representative spectral examples are shown in Figure 3. Seven of the nine differences observed involve NOEs with imidazole protons of His15. In addition, there is a new intraresidue NOE between the $C^{\beta}$ and $C^{\delta}$ protons of Arg17. The distance between these protons is governed by the dihedral angle $X_3$, and the longest these distances can become is ~3.5 Å (when $X_3 = 0°$), which is still within NOE range. Therefore, the absence of this NOE in unphosphorylated HPr is probably due to conformational averaging of the side chain. Observation of the $C^{\beta}H-C^{\delta}H$ NOE indicates that the Arg17 side chain exists in a more limited conformational range about $X_3$ in P-His15-HPr. A new strong NOE is observed between His15 $C^{\epsilon}H$ and Arg17 $C^{\beta}H$ in P-His15-HPr. In contrast, the cross peak between His15 $C^{\epsilon}H$ and Pro18 $C^{\gamma}H$ in NOESY spectra of the unphosphorylated form is not observed in the phosphorylated form.[4] The NOE differences are summarized on the *bs*HPr structure in Figure 4, and this representation indicates that the differences are likely due to a change in the disposition of the His15 imidazole ring relative to the rest of the active site. The changes in intraresidue His15 NOEs are consistent with the observation that $X_1$ of His15 is not altered and suggest a small rotation about $X_2$, moving the ring of His15 away from the side chains of Ser12 and Pro18 and toward the side chain of Arg17.

*Characterization of the Tautomeric States and Protonation States of His15.* Two-dimensional ($^1$H,$^{15}$N)-HMQC-*J* spectra of uniformly $^{15}$N-labeled proteins can be used to determine simultaneously the chemical shifts for both the carbon-bound protons and the nitrogens of imidazole side chains and to deduce the tautomeric state of the side chain (Van Dijk *et al.*, 1992; Pelton *et al.*, 1993). Figure 5 shows the relevant

[4] The resonance frequencies for Arg17 $C^{\beta}$ protons and Pro18 $C^{\gamma}$ protons are extremely close in unphosphorylated *bs*HPr. The identity of this cross peak was confirmed with a ($^1$H,$^{13}$C)-3D-NOESY-HMQC.

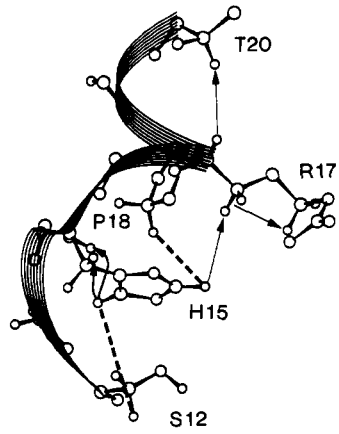


FIGURE 4: NOE changes observed upon phosphorylation on the structure of *bs*HPr. Residues 12−20 are shown. Protons are included only if they are involved in NOE changes. Dashed lines represent a reduction in intensity, and solid arrows indicate an increase in intensity as a result of phosphorylation.

region of HMQC-*J* spectra of *bs*HPr and P-His15-*bs*HPr. In these spectra, the $N^{\epsilon 2}$ resonances are easily identified by their strong correlations to both $C^{\epsilon 1}H$ and $C^{\delta 2}H$ resonances. Thus, in unphosphorylated HPr, the $N^{\epsilon 2}$ of His15 resonates at 176 ppm and the $N^{\delta 1}$ resonates at 242 ppm, indicating that $N^{\epsilon 2}$ is an α-type nitrogen and $N^{\delta 1}$ is a β-type nitrogen (Pelton *et al.*, 1993). In other words, in the neutral form of His15, the $N^{\epsilon 2}$ is protonated and the $N^{\delta 1}$ is not. Since the p$K_a$ of His15 is ~5.4, this will be the predominant species under physiological conditions.

Figure 5 also shows an HMQC-*J* spectrum for P-His15-*bs*HPr at pH 7.53. Again, the $N^{\epsilon 2}$ resonance is clear from its two strong cross peaks and is shifted significantly from its position in the spectrum of unphosphorylated HPr, from 176 to 230 ppm. $N^{\delta 1}$, the site of phosphorylation, shifts upfield to 203 ppm, as expected for $N^{\delta 1}$-phosphohistidine (van Dijk *et al.*, 1990). An HMQC-*J* spectrum of P-His15-*bs*HPr was also collected at pH 8.5 (data not shown). Comparison of the spectra collected at the two pH values showed that the $N^{\epsilon 2}$ resonance position is strongly dependent on pH between 7.53 and 8.5, consistent with a p$K_a$ of 7.8, as determined for P-His-HPr from *E. coli*, *Staphylococcus aureus*, and *Streptococcus faecalis* (Dooijewaard *et al.*, 1979; Kalbitzer *et al.*, 1982; Anderson *et al.*, 1993). The observation of a second weak cross peak correlating the $N^{\delta 1}$ and $C^{\delta 2}H$ in the spectra is also consistent with the phosphohistidine being in its imidazolium form over the pH range used (Pelton *et al.*, 1993). This second crosspeak is stronger in the spectrum acquired at pH 7.53, indicative of an increased population of protonated species at the lower pH. At neutral pH, significant populations of both species will exist.

Information concerning the involvement of histidine nitrogens in hydrogen bonding may be obtained indirectly from chemical shift values (van Dijk *et al.*, 1990) or may be obtained more directly via observation of slowly exchanging nitrogen-attached protons (Pelton *et al.*, 1993). On the basis of $^{15}N$ chemical shifts determined by direct-detect one-dimensional spectroscopy, van Dijk and co-workers concluded that the $N^{\epsilon 2}$ of His15 in *ec*HPr serves as an H-bond donor under neutral pH conditions, based on its 9.5 ppm downfield shift relative to imidazole. However, the solution structure of *ec*HPr does not contain a clear candidate for an H-bond involving the $N^{\epsilon 2}$ of His15 (van Nuland *et al.*, 1994). The His15 $N^{\epsilon 2}$ resonance is also shifted downfield in *bs*HPr, by 10 ppm relative to imidazole. There was, however, no detectable $N^{\epsilon 2}$−H cross peak in ($^1H$,$^{15}N$)-HMQC spectra collected using a 1-$\bar{1}$ echo water suppression on a sample dissolved in $H_2O$, indicating that this proton exchanges rapidly. Furthermore, in direct-detect, proton-coupled $^{15}N$ spectra of *bs*HPr collected at pH 7.0, the $N^{\epsilon 2}$ resonance appears as a singlet, indicating that the attached proton is exchanging at a rate in excess of the $^1J_{NH}$ coupling constant of ~90 Hz. Therefore, although the $N^{\epsilon 2}$ resonance in *bs*HPr is shifted downfield significantly, the NMR results do not offer direct evidence that this atom is involved in a hydrogen bond in solution.

In addition to the ionization of the imidazole nitrogen, the phosphoryl group in phosphohistidine can also exist in several ionization states. To ascertain the ionization state of the phosphoryl group, its $^{31}P$ resonance was followed as a function of pH. Spectra of P-His15-*ec*HPr contained three $^{31}P$ resonances, corresponding to inorganic phosphate (from the buffer), PEP, and P-His15. Figure 6 shows their dependence on pH over the range pH 4−10. Over this range, the inorganic phosphate and PEP each show a single ionization, with apparent p$K_a$s of 7.0 and 6.1, respectively. In contrast, the [$^{31}P$]P-His15 resonance exhibits a biphasic perturbation in chemical shift. The transition observed above neutral pH occurs over 2 pH units and therefore corresponds to a single ionization event. When linearized, these data yield a p$K_a$ of 7.8. Given the small magnitude of the pH-dependent transition at high pH (~0.7 ppm) and the fact that its apparent p$K_a$ is identical to that measured for the His15 $N^{\epsilon 2}$, we assign this $^{31}P$ perturbation to the protonation of the imidazolium rather than one of the phosphoryl oxygens. This transition was also detected in an earlier $^{31}P$ NMR study of *ec*HPr (Dooijewaard *et al.*, 1979). A $^{31}P$ perturbation of similar magnitude but opposite sign has been reported for the model compound $N^{\delta 1}$-phosphohistidine (Gassner *et al.*, 1977).

The $^{31}P$ transition observed below neutral pH is more complicated. It occurs over a broad pH range and is not yet complete at pH 4, where the solubility of the protein becomes limited. Such a broad transition indicates that the $^{31}P$ signal is responding to more than a single protonation event. Free $N^{\delta 1}$-phosphohistidine does not behave in a similar manner: its pH profile is completely flat between pH 8 and pH 4 and titrates steeply at lower pH (Gassner *et al.*, 1977). The profile for phosphoramidate is also flat between pH 6 and pH 4 with a transition below pH 4. These data suggest that, at pH values above neutral, the dianionic species of P-His15 is prevalent and that the broad transition observed below neutral pH corresponds to the protonation of two phosphoryl oxygens. Due to the insensitivity of the $^{31}P$ signal of $N^{\delta 1}$-phosphohistidine, experimentally determined values for the p$K_a$s of the phosphoryl oxygens are not readily available. The relevant p$K_a$ value for protonation of the dianionic species of phosphoramidate is 2.9 while the analogous p$K_a$ in phosphocreatine is 4.5 (Gassner *et al.*, 1977; Chase *et al.*, 1988). Thus, it appears that this ionization potential is quite sensitive to environment. The behavior observed in P-His15-HPr indicates that the dianionic species is strongly favored in the folded protein structure.

Taken together, the results reported in this section offer direct experimental evidence for the states of His15 in solution. These are shown in Figure 5. His15 exists in a

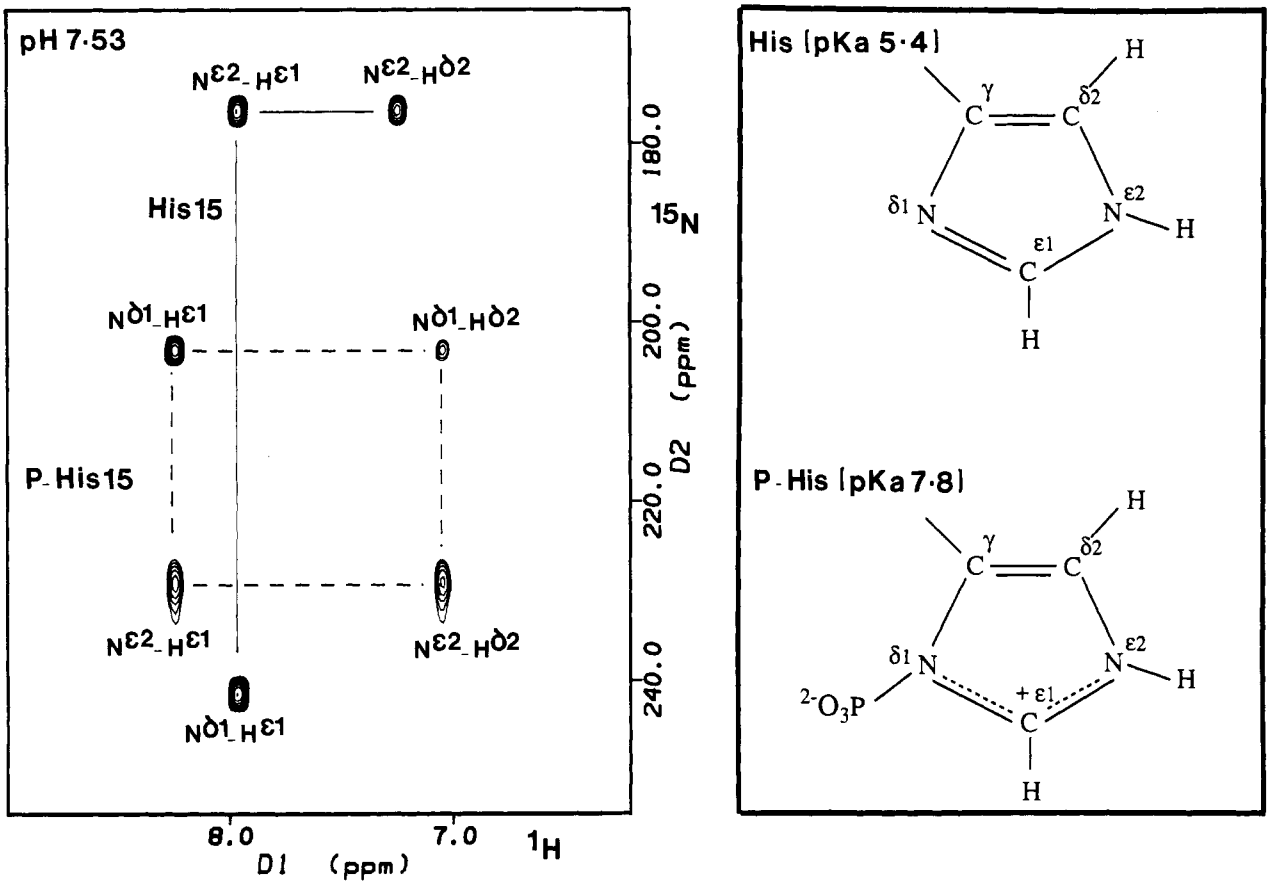


FIGURE 5: Portions of ($^1$H,$^{15}$N)-HMQC-*J* spectra of *bs*HPr (left) and the tautomeric states of the His15 ring before and after phosphorylation (right). Dashed lines connect resonances in P-His15, and solid lines connect resonances in the His15 ring. The spectra were collected at 22 °C and pH 7.53. The ring nitrogen and carbon-bound ring proton resonances are indicated.

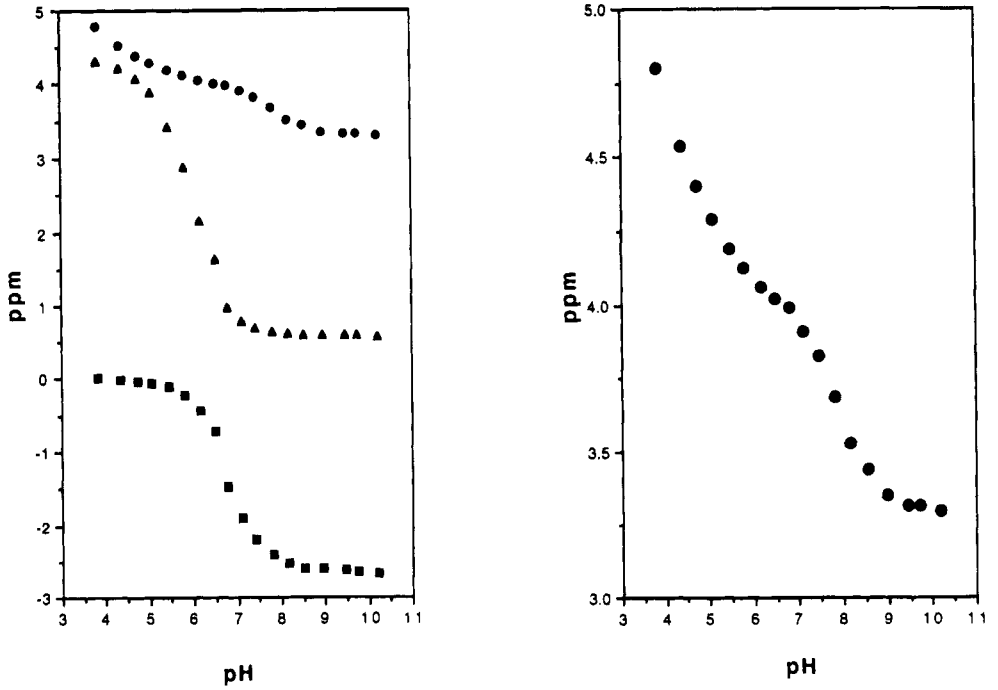


FIGURE 6: Dependence of $^{31}$P chemical shifts in P-His15-*ec*HPr on pH. Left: The bottom curve (squares) is for inorganic phosphate, the middle curve (triangles) is for PEP, and the top curve (circles) is for the resonance of P-His15. Right: The curve for the P-His15 resonance is expanded.

neutral form, with its $N^{\delta 1}$ unprotonated in the native protein. P-His15 exists as the imidazolium with a dianionic phosphoryl group, thus yielding a change in formal charge of −1 between the native and phosphorylated proteins.

*Involvement of Arginine-17 in P-His15-HPr.* Arg17 is invariant in all known HPrs, and it has been proposed that its side chain interacts specifically with the phosphoryl group of P-His15 (Herzberg *et al.*, 1992; Jia *et al.*, 1993a).

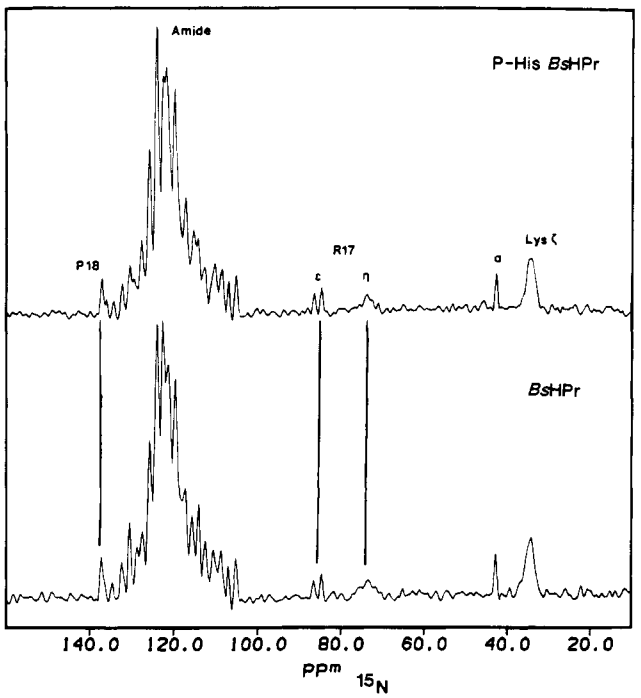


FIGURE 7: $^{15}N$ spectra of *bs*HPr and P-His15-*bs*HPr. The spectra were collected at 30 °C and pH 8.3. The regions where the different sets of resonances occur are shown as marked. Solid lines connect the Arg17 side-chain $N^{\epsilon}$ and $N^{\eta}$ resonances and the Pro18 $^{15}N$ in HPr before and after phosphorylation.

Substitution of Arg17 with a number of other amino acids has been shown to lower both the phospho-acceptor and phospho-donor activities of *ec*HPr (Anderson *et al.*, 1993). The solution structures of *bs*HPr and *ec*HPr do not show evidence for a direct interaction between His15 and Arg17, and the Arg17 side chain behaves as though it is conformationally flexible in the unphosphorylated forms of the proteins (Wittekind *et al.*, 1992; van Nuland *et al.*, 1994). The carbon-bound side-chain protons of Arg17 in P-His15-*bs*HPr (assigned from TOCSY spectra collected in $D_2O$) are not greatly perturbed from their original positions. However, as described above, changes are observed for Arg17 in both HNHB spectra and in NOESY spectra.

Since hypothesized interactions between the arginine side chain and the phosphohistidine residue involve the guanidinium group and the phosphoryl group, respectively, we attempted to obtain information directly on these functional groups. The nitrogen-bound protons of Arg17 were probed in a ($^1H$,$^{15}N$)-HMQC spectrum collected in $H_2O$ without a solvent presaturation pulse. The $N^{\epsilon}$ proton resonance was detected at pH 6.4, but the $N^{\eta}$ protons were not, presumably due to rapid exchange with solvent. The $N^{\epsilon}H$ resonance shifts very slightly downfield (~0.1 ppm) in P-His15-HPr. If one of the side-chain nitrogens were involved in an interaction with the negatively charged phosphoryl group as postulated, one might expect to observe a downfield shift of the corresponding $^{15}N$ resonance. The $^{15}N$ chemical shifts for the Arg17 side chain in both *bs*HPr and P-His15-*bs*HPr were determined from direct-detect $^{15}N$ 1D spectra (Figure 7). Assignment of the resonances was straightforward because Arg17 is the only arginine in HPr. $^{15}N$ spectra were collected at several different pH values (pH 6.4, 7.0, 8.3), and the $^{15}N$ chemical shifts for the unphosphorylated and phosphorylated proteins were indistinguishable in all cases. This observation would seem not to indicate involvement of Arg17 in an H-bond. We note, however, that the $^{15}N$ chemical shift for the $N^{\epsilon}$ of an arginine that is known to be involved in an H-bond to a carboxylate in a zinc finger peptide is not shifted downfield, although in this case its attached proton ($N^{\epsilon}H$) is shifted downfield by ~1.5 ppm (Rajagopal, Heese, and Klevit, unpublished observation).

Even though the nitrogens of Arg17 do not seem to sense the presence of the phosphoryl group, the $^{31}P$ resonance of P-His15 senses the presence of the arginine side chain. This conclusion is based on the $^{31}P$ chemical shift observed for the phosphorylated form of a mutant *ec*HPr in which Arg17 is replaced with a lysine. Over the range of pH 4−10, the $^{31}P$ signal for R17K is shifted downfield relative to the wild-type spectrum (data not shown). The largest difference in chemical shift observed between the wild type and mutant is ~1.3 ppm and occurs at pH values greater than 7. The smallest measured difference is ~0.3 ppm, which occurs at the low end of the pH titration, at ~pH 4. This observation indicates that the chemical environment of the dianionic species of P-His15 is more sensitive than the protonated species to the proximity of Arg17.

## DISCUSSION AND CONCLUSIONS

P-His15-HPr is an important intermediate along the PTS pathway. It also serves as an example of a protein that is phosphorylated on the $N^{\delta 1}$ atom of a histidine. We have therefore characterized this species to ascertain the extent and nature of structural changes associated with phosphorylation. Taken together, the chemical shift perturbations, coupling constants, NOE data, and amide exchange rates indicate that phosphorylation of His15 is accompanied by a small change in local conformation. The most significant effects involve the side chains of His15 and Arg17.

The NOE data indicate a change in the disposition of the His15 ring. When $N^{\delta 1}$-phosphohistidine was substituted for His15 in the *bs*HPr structure (see Materials and Methods), a steric clash between two phosphoryl oxygens and the main-chain amide protons of residues 16 and 17 occurred. The unfavorable distances could be relieved by a rotation about $X_2$ of His15 of as little as ~10−15°. Such a rotation also gave qualitative agreement with the NOE changes observed for His15 and moved the two phosphoryl oxygens into favorable positions relative to NH16 and NH17. Herzberg and colleagues incorporated a small rotation about $X_2$ in their model building of P-His15-*bs*HPr (Herzberg *et al.*, 1992). The NMR data presented here serve as experimental confirmation of that proposal. Residues 16 and 17 are the first two residues in an α-helix, and their rapid exchange rates in unphosphorylated *bs*HPr are consistent with these amides not serving as H-bond donors in that form of the protein. The large downfield shifts and decreased exchange rates observed for these two amide groups are strong evidence for their involvement as H-bond donors in P-His15-HPr. As illustrated in Figure 8, substitution of P-His15 in the *bs*HPr structure produces a model in which two phosphoryl oxygens are proximal to the amides in question. Thus, although the NMR measurements themselves cannot directly identify hydrogen bond acceptors, the observations presented here indicate that the best candidates for NH16 and NH17 in P-His15 are phosphoryl oxygens. The $^{31}P$ spectra of P-His15-HPr indicate that the phosphoryl group is in the dianionic form under physiological conditions. This nega-

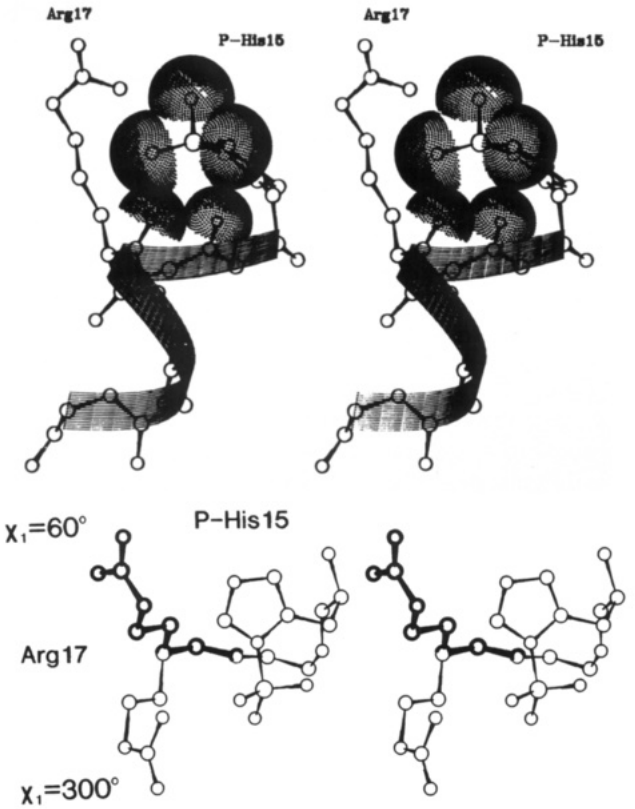


FIGURE 8: Model for P-His15-*bs*HPr. (A, top) P-His15 is in the N-cap position at the N-terminal end of α-helix A in HPr (residues 16−27). A small rotation about $X_2$ results in favorable distances between phosphoryl oxygens and the main-chain amide groups of residues 16 and 17. Also, the side chain of Arg17 is shown in its $X_1 = 300°$ conformation. (B, bottom) Models for P-His15-*bs*HPr in which Arg17 $X_1 = 60°$ and 300° are superimposed to illustrate the difference in the position of the guanidinium group generated by this difference in side-chain dihedral angle.

tively charged group is therefore situated to allow for favorable electrostatic interaction by virtue of its position at the N-terminal end of the α-helix.

The new intraresidue NOEs and HNHB coupling pattern observed for Arg17 in the phosphorylated form indicate that this side chain has become more limited in its conformational range, and these data are consistent with Arg17 existing primarily as a single rotamer with $X_1$ = either 60° or 300°. The new interresidue NOE between His15 $C^\epsilon H$ and an Arg17 $C^\beta$ proton allows us to distinguish between the two possibilities. For $X_1 = 60°$, the distances between the His15 $C^\epsilon$ proton and the two $C^\beta$ protons of Arg17 are 4.3 and 4.9 Å, outside the range where one would expect to observe NOEs at short mixing times. On the other hand, for $X_1 = 300°$, the relevant distances are 3.3 and 4.8 Å.[5] Thus, the NOE data are more consistent with Arg17 existing in a conformation with $X_1$ near 300°. As shown in Figure 8, the two Arg17 side-chain conformations yield very different positions of the guanidinium group of Arg17 in a model of P-His15-*bs*HPr. The $X_1 = 60°$ rotamer has its guanidinium group pointing away from the phosphoryl group, while the $X_1 = 300°$ rotamer has the functional group pointing toward the phosphoryl group. Thus, the NMR data are most consistent with a model in which the side chain of Arg17 becomes more restricted in P-His15-HPr, taking on a conformation that places it in a position to allow for a favorable electrostatic interaction between the guanidinium group and the phosphoryl group. Such a favorable interaction must overcome the entropic cost associated with the more limited conformational behavior of the Arg17 side chain.

In crystals of *bs*HPr and *ec*HPr grown from high concentrations of ammonium sulfate, a sulfate ion is present at the active site which has been suggested to serve as a serendipitous model for the phosphoryl group (Herzberg *et al.*, 1992; Jia *et al.*, 1993). However, the exact position of the sulfate is different in the two structures, which may be a consequence of the different ionization states of His15 in the two crystals. In the *bs*HPr crystal, the sulfate does not interact directly with His15, but rather with the Arg17 side chain and with groups on two neighboring molecules in the protein crystal. The model proposed by Herzberg and colleagues for P-His15-*bs*HPr retains the interaction between the phosphoryl group and the guanidinium group of Arg17 and incorporates interactions with the two main-chain amides from Ala16 and Arg17. In the *ec*HPr crystal structure, the sulfate ion is closer to the protonated His15 side chain, with two of the sulfate oxygens being within 3 Å of the $N^{\delta 1}$ of the imidazole. The sulfate also interacts with the main-chain amide nitrogens of 16 and 17 in the *ec*HPr structure. In contrast, the side chain of Arg17 points away from the sulfate ion and is instead involved in one intramolecular interaction and one intermolecular interaction. Thus, both models predicted that phosphoryl oxygens of P-His15 would interact with the amides of residues 16 and 17, consistent with the NMR results reported here. The distinguishing feature of the two models is the position of the guanidinium group of Arg17. The NMR results favor a model in which an interaction between Arg17 and the phosphoryl group exists. Neither of the crystal structures has the Arg17 $X_1$ of 300°, as indicated in solution, although Herzberg and colleagues mention that a rotation in Arg17 $X_1$ of 40° was incorporated in their model, yielding a $X_1$ of either 140° or 220° in their model (the direction of the rotation was not specified). Therefore, although certain general features of the P-His15-HPr structure are well predicted by the models, some details may not be accurate. This is in keeping with structural studies involving binding of sulfate and phosphate ions that have shown that while the two groups may bind to the same site on a protein, the details of the interactions observed can be quite different (Jacobson *et al.*, 1988; Verlinde *et al.*, 1991).

The strength and the role of the putative interaction involving Arg17 cannot be judged from the NMR data. Such an interaction may serve to stabilize the phosphorylated form of HPr. Other possible roles for the conserved Arg17 include (1) a role in the transition state of phosphotransfer from His15 in HPr to the active His in EIIA and (2) a specific interaction between Arg17 and one of the conserved Asp residues in EIIA (Herzberg, 1992). A series of Arg17 mutants in *ec*HPr showed larger effects on $K_m$ than on $V_{max}$ in their reactions with several EIIAs (Anderson *et al.*, 1993)—a result that is more consistent with the second of the two proposals. These proposals can be tested in future studies in which the

[5] The distances between the His15 $C^\epsilon$ proton and the two Arg17 $C^\beta$ protons are dependent on the $X_2$ of His15, as well as the $X_1$ of Arg17. The closest distance when Arg17 $X_1$ is 60° is 3.7 Å, which occurs when the $X_2$ of His15 is ~90°, which results in steric clashes between the phosphoryl oxygens and several main-chain atoms.

interaction between HPr and EIIA is studied directly using solution NMR techniques.

The solution NMR results unambiguously reveal the tautomeric and ionic states of His15 in both unphosphorylated and phosphorylated HPr, as pictured in Figure 5. In the solution structure of *bs*HPr, $N^{\delta 1}$ faces the solvent and $N^{\epsilon 2}$ faces the interior of the protein. At neutral pH, $N^{\delta 1}$ is not protonated, leaving it poised for nucleophilic attack on phosphorylated EI. In P-His15-HPr, the imidazolium form is prevalent, but a significant proportion of the unprotonated form will also exist. The imidazolium form should be the more reactive species, and upon nucleophilic attack by the active histidine in EIIA and cleavage of the N−P bond, the neutral form of His15 could be regenerated without requiring a proton donor. Hydrolysis of P-His15-HPr is likely to proceed by an analogous mechanism, and the reported pH dependence of the rate of phosphohydrolysis, which increases as the pH is decreased through the imidazolium $pK_a$ of 7.8, is consistent with this proposal (Waygood *et al.*, 1985).

Until recently, histidine phosphorylation was thought to be an unusual event found only in prokaryotic systems, such as the PTS. However, a growing number of examples of histidine phosphorylation have been reported in eukaryotic systems in recent years, and both histidine kinases and histidine phosphatases have been described (Hughes, 1994; Motojima & Goto, 1994). At present, very little is known at a molecular level about these systems. Thus, the PTS is an excellent system in which to study the effects of histidine phosphorylation on protein structure. The ramifications of phosphorylation of the active site His90 residue in $III^{glc}$ (also known as $EIIA^{glc}$) from *E. coli*, the protein that serves as the phosphoacceptor for *ec*HPr, have also been studied by NMR (Pelton *et al.*, 1992). Similar to the results reported here for HPr, chemical shift perturbations were only observed for residues that are in close proximity to His90, and a very limited number of NOE differences were detected between the unphosphorylated and phosphorylated protein. On the basis of these results, the authors concluded that phosphorylation of His90 results in very minor conformational changes. It is interesting to note that the NOEs indicated a slight movement of the imidazole ring of His90 toward a nearby main-chain amide proton, that of Asp94. On the basis of the crystal structure of unphosphorylated $III^{glc}$, Worthylake *et al.* (1991) had proposed that the amides of residues 94 and 95 might interact with phosphoryl oxygens of the phosphohistidine. Indeed, similar to the results reported here for P-His15-HPr, Pelton *et al.* (1993) observed decreased amide proton exchange rates for Asp94 and Thr95, the first two residues in helix II in phosphorylated $III^{glc}$.

Thus, the NMR results indicate that P-His15-HPr and P-His90-$III^{glc}$ may employ a similar mechanism for stabilizing the phosphohistidine moiety, in which the negatively charged phosphoryl oxygens form H-bonds to backbone amide protons at the N-terminal end of a nearby α-helix in the protein structure. It remains to be seen how general this mechanism will be. However, the placement of phosphoryl groups near the N-terminal ends of α-helices is a theme that has already been identified in proteins that bind phosphoryl moieties noncovalently. The ability to perform detailed NMR studies in solution on these short-lived phosphorylated proteins should yield atomic-level information regarding the structural ramifications of phosphorylation of histidine residues on other systems in the future.

## ACKNOWLEDGMENT

We thank Jonathan Reizer for his gift of the overexpression system for *bs*HPr, Sandra Y. Lee for performing the $^{31}P$ NMR experiments, Peter Brzovic for preparing Figure 1, and L. T. J. Delbaere for providing the coordinates for *ec*HPr prior to their release.

## REFERENCES

Anderson, J. W., Waygood, E. B., Saier, M. H. J., & Reizer, J. (1992) *Biochem. Cell Biol. 70*, 242−246.
Anderson, J. W., Pullen, K., Georges, F., Klevit, R. E., & Waygood, E. B. (1993) *J. Biol. Chem. 268*, 12325−12333.
Archer, S. J., Ikura, M., Torchia, D. A., & Bax, A. (1991) *J. Magn. Reson. 95*, 636−641.
Bax, A., & Davis, D. G. (1985) *J. Magn. Reson. 65*, 355−360.
Bax, A., Ikura, M., Kay, L. E., Torchia, D. A., & Tschudin, R. (1990) *J. Magn. Reson. 86*, 304−318.
Bodenhausen, G., Kogler, H., & Ernst, R. R. (1984) *J. Magn. Reson. 58*, 370−388.
Chase, B., *et al.* (1988) *Biophys. J. 53*, 935.
Chen, Y., Reizer, J., Saier, M. H., Jr., Fairbrother, W. J., & Wright, P. E. (1993) *Biochemistry 32*, 32−327.
Dooijewaard, G., Roosien, F. F., & Robilliard, G. T. (1979) *Biochemistry 18*, 2996−3001.
Fairbrother, W. J., Cavanagh, J., Dyson, H. J., Palmer, A. G., III, Sutrina, S. L., Reizer, J., Saier, M. H., Jr., & Wright, P. E. (1991) *Biochemistry 30*, 6896−6907.
Gassner, M., Stehlik, D., Schrecker, O., Hengstenberg, W., Maurer, W., & Ruterjans, H. (1977) *Eur. J. Biochem. 75*, 287−96.
Hammen, P. K., Waygood, E. B., & Klevit, R. E. (1991) *Biochemistry 30*, 11842−11850.
Herzberg, O. (1992) *J. Biol. Chem. 267*, 24819−24823.
Herzberg, O., Reddy, P., Sutrina, S., Saier, M. H., Jr., Reizer, J., & Kapadia, G. (1992) *Proc. Natl. Acad. Sci. U.S.A. 89*, 2499−2503.
Jacobson, B. L., & Quiocho, F. A. (1988) *J. Mol. Biol. 204*, 783−787.
Jia, Z., Quail, J. W., Waygood, E. B., & Delbaere, L. T. (1993a) *J. Biol. Chem. 268*, 22490−22501.
Jia, Z., Vandonselaar, M., Quail, J. W., & Delbaere, L. T. (1993b) *Nature 361*, 94−97.
Jia, Z., Vandonselaar, M., Hengstenberg, W., Quail, J. W., & Delbaere, L. T. (1994) *J. Mol. Biol. 236*, 1341−1355.
Kalbitzer, H. R., Neidig, K. P., & Hengstenberg, W. (1991) *Biochemistry 30*, 11186−11192.
Klevit, R. E., & Waygood, E. B. (1986) *Biochemistry 25*, 7774−7781.
Kraulis, P. J. (1991) *J. Appl. Crystallogr. 24*, 946−950.
Marion, D., & Wüthrich, K. (1983) *Biochem. Biophys. Res. Commun. 113*, 967−974.
Marion, D., Ikura, M., Tschudin, R., & Bax, A. (1989) *J. Magn. Reson. 85*, 393−399.
Mueller, L. (1987) *J. Magn. Reson. 72*, 191−196.
Pelton, J. G., Torchia, D. A., Meadow, N. D., & Roseman, S. (1992) *Biochemistry 31*, 5215−5224.
Pelton, J. G., Torchia, D. A., Meadow, N. D., & Roseman, S. (1993) *Protein Sci. 2*, 543−558.
Peng, J. W., & Wagner, G. (1992) *J. Magn. Reson. 98*, 308−332.
Postma, P. W., Lengeler, J. W., & Jacobson, G. R. (1993) *Microbiol. Rev. 57*, 543−594.
Redfield, A. G., & Papastavros, M. Z. (1990) *Biochemistry 29*, 3509−3514.
Reizer, J., Sutrina, S. L., Wu, L. F., Deutscher, J., Reddy, P.,

& Saier, M. H., Jr. (1992) *J. Biol. Chem. 267*, 9158−9169.
Sklenar, V., & Bax, A. (1987) *J. Magn. Reson. 74*, 469−479.
Spera, S., Ikura, M., & Bax, A. (1991) *J. Biomol. NMR 1*, 155−165.
States, D. J., Haberkorn, R. A., & Ruben, D. J. (1982) *J. Magn. Reson. 48*, 286.
Sutrina, S. L., Reddy, P., Saier, M. H., Jr., & Reizer, J. (1990) *J. Biol. Chem. 265*, 18581−18589.
van Dijk, A. A., Scheek, R. M., Dijkstra, K., Wolters, G. K., & Robillard, G. T. (1992) *Biochemistry 31*, 9063−9072.
van Nuland, N., van Dijk, A. A., Dijkstra, K., van Hoesel, F., Scheek, R. M., & Robillard, G. T. (1992) *Eur. J. Biochem. 203*, 483−491.
van Nuland, N., Hangyi, I. W., van Schaik, R. C., Berendsen, H. J., van Gunsteren, W. F., Scheek, R. M., & Robillard, G. T. (1994) *J. Mol. Biol. 237*, 544−559.
Verlinde, C. L., Noble, M. E., Kalk, K. H., Groendijk, H., Wierenga, R. K., & Hol, W. G. (1991) *Eur. J. Biochem. 198*, 53−57.
Waygood, E. B., Erickson, E., el-Kabbani, O. A., & Delbaere, L. T. (1985) *Biochemistry 24*, 6938−6945.
Wittekind, M. G., & Klevit, R. E. (1991) NMR Studies of Two Related Phosphotransfer Proteins, in *Expanding Frontiers in Polypeptide and Protein Research*, ESCOM, The Netherlands.
Wittekind, M., Reizer, J., & Klevit, R. E. (1990) *Biochemistry 29*, 7191−7200.
Wittekind, M., Rajagopal, P., Branchini, B. R., Reizer, J., Saier, M. H., Jr., & Klevit, R. E. (1992) *Protein Sci. 1*, 1363−1376.
Worthylake, D., Meadow, N. D., Roseman, S., Liao, D. I., Herzberg, O., & Remington, S. J. (1991) *Proc. Natl. Acad. Sci. U.S.A. 88*, 10382−10386.
Wüthrich, K. (1986) *NMR of Proteins and Nucleic Acids*, John Wiley & Sons, Inc., New York, NY.